Study of Fault Conditions During Heat Treatment of Nb_3Sn Strand

Yunfei Tan, Xiangyang Wu, Wenge Chen, Donghui Jiang, Guihong Zou, Zhen Fang, Zhangyang Liu, Yang Gao, Zhiyou Chen, and Guangli Kuang

***Abstract*—Heat treatment of large-scale superconducting coils is limited by the power of the furnace and the weight of the superconducting coils. For the superconducting coils to be used in a 45-T hybrid magnet, the practical temperature curve will lag behind the setting temperature curve, particularly for the lowest temperature stage (210 °C). There is also a risk that the heat treatment might be interrupted due to a general power failure or equipment failure. The highest temperature stage (640 °C) is the key stage to form Nb_3Sn crystals; thus, interruption of the heat treatment during the 640 °C stage is expected to cause a great impact on the performance of a Nb_3Sn superconducting magnet. This paper compares the performance of Nb_3Sn strand samples given the recommended heat treatment with samples subjected to simulated temperature lag or simulated power failure. All of the samples had Residual Resistance Ratios, critical currents, and calculated heat losses that were satisfactory for use in the superconducting part of the 45-T hybrid magnet.**

***Index Terms*—Critical current, heat treatment, Nb_3Sn, superconducting coils.**

I. Introduction

A 45 T hybrid magnet is being constructed in the High Magnetic Field Laboratory, Chinese Academy of Sciences (CHMFL) [1]–[4], the superconducting magnet of the hybrid magnet will use Nb_3Sn superconducting strand and will provide an 11 T central field. The superconducting magnet consists of six superconducting sub-coils. A large, vertical type, vacuum/argon-atmosphere-protected, heat treatment system has been constructed to heat treat the superconducting sub-coils [5]. The heat treatment furnace has been designed to be operated in two modes: vacuum and atmosphere-protection. It can be switched directly from one mode to the other during the heat treatment process. The working volume of the furnace is Ø2000 mm × 2500 mm tall, but each sub-coil still has to be heat treated individually due to the its large weight (1.7 to 2.7 tons for each sub-coil).

An obvious artifact was observed during the heat treatment of the superconducting sub-coils. The temperatures of some monitor points were obviously behind a few dozen degrees when other temperature monitoring points arrived at the setting temperature, especially for the lowest temperature stage (210 °C). This is mainly because the sub-coil was heated by radiant heat from the furnace and the heating efficiency of radiant heat is very low at low temperature. The slowest temperature point lags 20 to 30 hours behind the fastest temperature point. The low temperature stage of the heat treatment is the Cu-Sn diffusion stage in the superconductor, so a potential worry is the influence of this temperature lag on the physical performance of the large-scale superconducting magnet.

The heat treatment of each superconducting sub-coil will last about one month from the preparation to the end, so the furnace will work continuously for six months to treat all six superconducting coils. The heat treatment might be interrupted due to power failure, equipment failure or other fault condition. If the power failure lasts long enough, the vacuum of the furnace will be destroyed, and the temperature will ramp down. The furnace can be restarted after the fault is repaired; however, changes to the heat treatment process due to heat interruption are likely to affect the physical parameters of the superconducting coils in the furnace and thus affect RRR and I_c. The changes to the coils will depend on where in the heat treatment process the interruption occurred.

In the study reported here, we prepared some Nb_3Sn samples to be heat treated according to the two fault conditions described above: temperature lag and treatment interruption. Then the RRR, I_c, and magnetization of the strands were studied to verify the influences of the heat treatment fault conditions on the performance of the large-scale superconducting magnet.

II. Sample Preparation

The strand under study was a Ti-doped restacked-rod process (RRP) Nb_3Sn wire made by Oxford Instruments Superconducting Technology (OST) [6], [7], the specifications of the strand are listed in Table I and a cross-section picture of the strand is shown in Fig. 1. The OST recommended heat treatment schedule for optimum I_c and RRR is 210 °C/48 hr + 400 °C/48 hr + 640 °C/60 hr + ramp down to 500 °C, followed by a cool down to room temperature. The ramp rate is 10 °C/hr for all steps except during the cool down where the furnace is cooled at no preset rate.

Manuscript received October 19, 2015; accepted January 18, 2016. Date of publication January 20, 2016; date of current version February 9, 2016. This work was supported by the National Natural Science Foundation of China under Grant U1232143, by the Youth Innovation Promotion Association, by the CAS under Grant 2013210, by the CAS Key Technology Talent program, and by the Special Project of the Ministry of Science and Technology of China under Grant 2014GB125001.

Y. Tan, W. Chen, D. Jiang, G. Zou, Z. Chen, and G. Kuang are with the Chinese High Magnetic Field Laboratory, Chinese Academy of Sciences, Hefei 230031, China (e-mail: tanyf@ipp.ac.cn).

X. Wu, Z. Fang, Z. Liu, and Y. Gao are with the Chinese High Magnetic Field Laboratory, Chinese Academy of Sciences, Hefei 230031, China, and also with the University of Science and Technology of China, Hefei 230026, China.

Color versions of one or more of the figures in this paper are available online at http://ieeexplore.ieee.org.

Digital Object Identifier 10.1109/TASC.2016.2519892

TABLE I
SPECIFICATION OF THE Nb_3Sn STRAND

Superconducting Wire	Nb_3Sn
Diameter	0.81 mm
Cr coating thickness	~ 2 μm
Filament diameter	< 70 μm
J_c at 10 μV/m	≅ 2100 A/mm^2(12 T, 4.2 K)
Cu/non-copper	1.0
n-value	≅20 (12 T, 4.2 K)
RRR	≅ 100
Hysteresis loss	< 1600 mJ/cm^3(7 T-0-7 T)
Twist pitch	15 mm

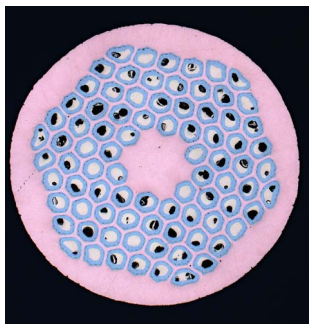

Fig. 1. Cross-section of a heat treated Ti-doped restacked-rod process (RRP) Nb_3Sn wire.

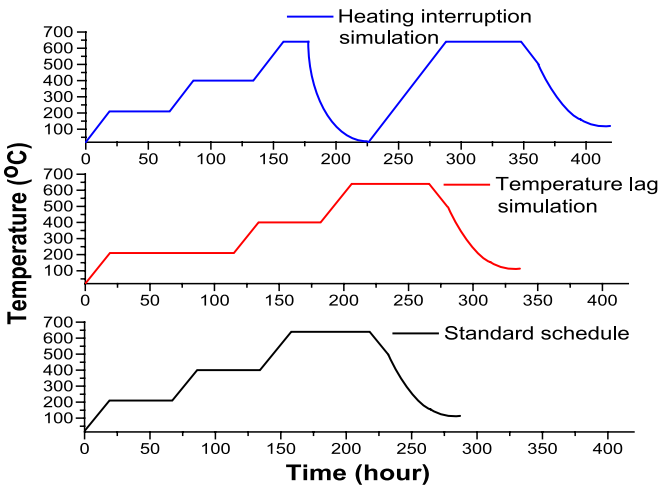

Fig. 2. Schematic diagram of standard heat treatment and fault conditions.

The temperature lag simulation extended the heating time from 48 hr to 96 hr during the 210 °C stage. The power interruption simulation stopped the heating of the furnace after 20 hours at 640° and turned off the vacuum pump. The temperature decreased to room temperature and the system gradually filled with air; then the furnace was evacuated to restore the vacuum and the temperature was recovered to 640 °C to accomplish the remaining 40 hours heat treatment. Schematic diagrams of the standard heat treatment and the two simulated fault conditions are shown in Fig. 2.

Samples were prepared for RRR, I_C, and magnetization measurements with different heat treatment conditions. For the critical current sample, the Cr plating was removed from the surface of the strand by chemical etching in a solution of HCl

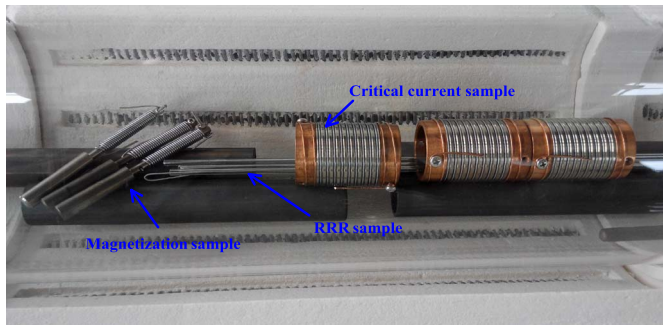

Fig. 3. Nb_3Sn strand samples in the heat treatment furnace.

TABLE II
TEST RESULTS OF CRITICAL CURRENT SAMPLES

Heat treatment condition	I_c Sample Number	I_c (A) 12 T	14 T	16 T
Standard schedule	1	561	364	221
	2	578	377	225
Temperature lag simulation	3	581	382	232
	4	572	375	222
Heating interruption simulation	5	None	357	219
	6	558	360	218

acid, and the strand was wound on a Ti-6Al-4V standard ITER sample barrel. For the RRR sample, the Cr plating was not removed from the strand section between the voltage taps. Each sample was a straight, 10–20 mm strand section that was cut from near the strand end after heat treatment to avoid the influence of end effects on the strand performance (e.g., due to Sn outflow). Because the shape of the strand sample would influence the magnetization measurements, we wound the strand sample on a spiral with 5 mm inner diameter and 1 mm pitch. After the heat treatment, a section of the spiral was cut and used as a hysteresis loss sample.

All three kinds of sample were heat treated together for the same heat treatment conditions. The samples for the standard heat treatment conditions and two fault conditions were prepared in a vacuum quartz tube furnace. The strand samples in the furnace are shown in Fig. 3.

III. EXPERIMENTAL MEASUREMENTS

A. Critical Current Test

The critical current was defined at an electric-field criterion of 10 μV/cm. The voltage signal from a pair of voltage taps 500 mm apart was recorded. The self field of the coiled sample was not taken into account in this study. I_C was measured at 4.2 K in background magnetic fields from 12 T to 15 T. All the I_C data can satisfy the requirements of a 45 T hybrid magnet except one measurement at 12 T that was rejected due to local mechanical movement of the sample. The critical current results are listed in Table II and also shown in Fig. 4. The I_C test results of different heat treatments differ by less than 7%. This implies that a time extension at the lowest temperature stage will have little influence on the I_C performance of the large-scale superconducting magnet. Also, an interruption of the heat treatment at the final temperature stage will not be

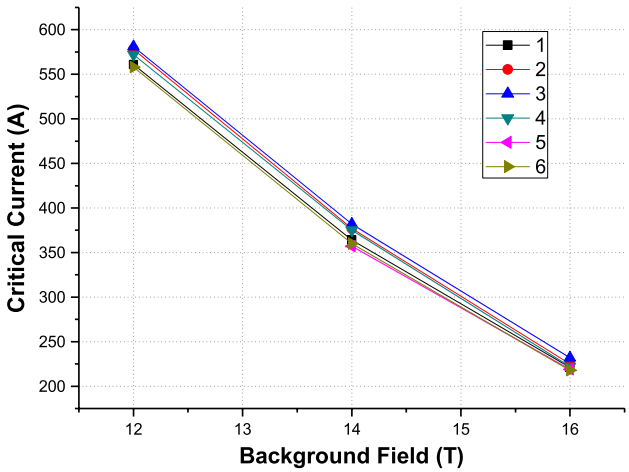

Fig. 4. Critical current test results of different heat treatment sample versus magnetic field.

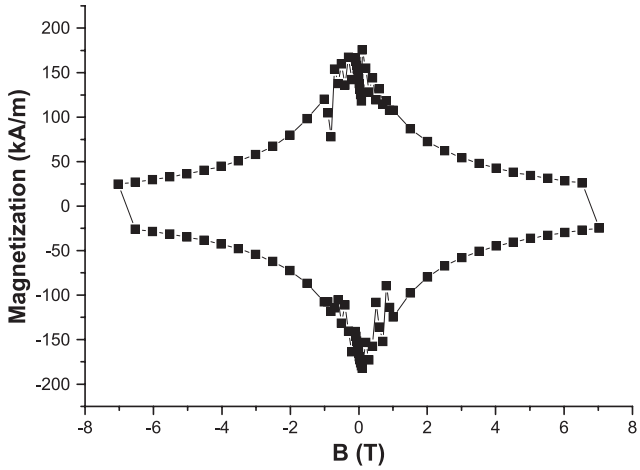

Fig. 5. Magnetization loop of the tested Nb_3Sn sample.

TABLE III
TEST RESULTS OF RRR SAMPLES

Heat treatment condition	RRR Sample Number	RRR value
Standard schedule	1	115.2
	2	143.1
	3	163.6
Temperature lag simulation	4	135.1
	5	137.9
	6	140.5
Heating interruption simulation	7	119.1
	8	131.3
	9	132.8

fatally dangerous and can be recovered from for the large-scale superconducting magnet.

B. Residual Resistivity Ratio (RRR) Measurements

The sample resistance was measured at 0 °C with $I = 1$ A. Then the sample resistance was measured with constant current (1 A) and decreasing temperature until the superconducting transition onset (17–18 K @ 0 T) appeared. The RRRs, defined as the ratios of the two resistance measurements, are listed in Table III. At either the Cu-Sn diffusion stage or the Nb_3Sn forming stage, changes to either the reaction temperature or the reaction time will affect the Sn diffusion, which may affect the RRR. However, it is obvious from Table III that neither the change of the reaction time due to the temperature lag nor the heating interruption due to power or control system failure changed the RRR too much. All the RRR values are larger than 100, which can satisfy the specification of the Nb_3Sn strand.

C. Magnetization Measurements

The magnetization loop of the samples was measured by a commercial magnetometer. The samples were cycled from −7 T to 7 T. An obvious flux jump was observed from the test results shown in Fig. 5 at fields less than 1.5 T. The flux jump will result in magnetic instability at low field. The stability current density, above which flux jumps can quench the strand, was correlated with strand RRR. A low RRR of 5 to 10 can drop the stability current density below I_C at 12 T [8], which will limit the performance of the superconducting magnet due to a possible quench in the low field sections.

TABLE IV
CALCULATED HYSTERESIS LOSS OF MAGNETIZATION SAMPLES

Heat treatment condition	Magnetization Sample Number	Hysteresis loss (mJ/cm^3) (7T-0-7T)
Standard schedule	1	1747
	2	1769
Temperature lag simulation	3	1716
	4	1764
Heating interruption simulation	5	1738
	6	1736

The DC magnetization loop was reconstructed by interpolation of the measured points. The hysteresis loss was calculated from the area of the M(B) loop [9]. The magnetization loops of all the samples were the same within 3%. The calculated hysteresis losses for −7 T-0-7 T are shown in Table IV; they are a little higher than the required specifications shown in Table I.

IV. HEAT TREATMENT OPTIMIZATION FOR THE LARGE-SCALE SUPERCONDUCTING MAGNET

The heat treatment is the key process to form superconducting crystals of Nb_3Sn [10], [11]. Unlike the ductile alloys of NbTi, Nb_3Sn is a kind of brittle intermetallic compound. The entire superconducting coil made of Nb_3Sn strand must undergo high temperature heat treatment to form the Nb_3Sn compound. The heat treatment temperature and time will directly affect the performance of the superconducting magnet. Because the heating power via radiant heat is proportional to the fourth power of the temperature, temperature lag is unavoidable for large-scale superconducting coils at lower temperature stages, especially for the 210 °C stage (see Fig. 6).

The heat treatment schedule for the Nb_3Sn supplied by the OST was optimized to meet the desired specifications of the strand. The heat treatment of the large-scale superconducting coils should follow the schedule specified for the strand. We will arrange more than 20 temperature sensors in different

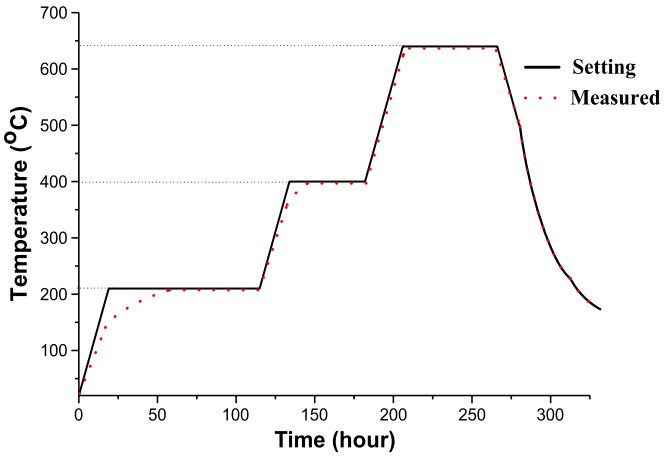

Fig. 6. Heat treatment schedule of the large-scale superconducting magnet. The plain line is the setting schedule, and the dotted line is the measured schedule.

positions on the superconducting coils to monitor the temperature evolution during heat treatment. We will adjust the times of the lower temperature stages (210 °C and 400 °C) according to the real time measurement results of the temperature to ensure that all parts of the superconducting coils will be at the desired temperatures for 48 hours.

The 640 °C stage is the most critical for forming Nb_3Sn compound. Temperature lags at this stage are not obvious due to the high temperature. We will control the temperature fluctuation to be less than ±2.5 °C and ensure that the heating time is at least 50 hours and not more than 70 hours. If the heat treatment is stopped by equipment failure or power failure, the furnace and the coil being heat-treated will cool to room temperature on their own. After the failure is eliminated, heat treatment can be resumed from the moment at which it stopped. The superconducting coils will accomplish the remaining heat treatment according to the standard schedule.

V. Conclusion

The effects of two kinds of heat treatment fault conditions were simulated for a large-scale superconducting magnet made of OST RRP Nb_3Sn samples. The Nb_3Sn strands were not vulnerable to the heat treatment fault conditions. The samples had high I_C performance, high RRR values, and low hysteresis loss even when the duration of the lowest temperature stage was doubled or the final temperature stage was ramped down to room temperature and then recovered. The I_C and RRR fully met the strand specification. The calculated hysteresis loss was a little high, but was the same as that attained with the standard schedule. Therefore, the heat treatment schedule of the large-scale superconducting magnet can be optimized to adapt to the actual working conditions, including the risk of equipment failure or power failure. Even a temperature lag at the lowest temperature stage or a temperature interruption at the final temperature stage will have a negligible effect on the I_C, RRR, and hysteresis losses.

References

[1] G. Kuang, "A 40 T hybrid magnet under construction in china," *IEEE Trans. Appl. Supercond.*, vol. 20, no. 3, pp. 680–683, Jun. 2010.
[2] Y. Tan *et al.*, "Cable-in-conduit conductor fabrication for the hybrid magnet of CHMFL," *IEEE Trans. Appl. Supercond.*, vol. 25, no. 3, Jun. 2015, Art. ID 4600204.
[3] Y. Tan, W. Chen, F. Xu, and J. Zhu, "Thermal-hydraulic performance analysis of the superconducting magnet during the trip of the resistive magnet in CHMFL hybrid magnet," *IEEE Trans. Appl. Supercond.*, vol. 24, no. 3, Jun. 2014, Art. ID 4300404.
[4] W. G. Chen *et al.*, "Final design of the 40 T Hybrid magnet superconducting outsert," *IEEE Trans. Appl. Supercond.*, vol. 23, no. 3, Jun. 2013, Art. ID 4300404.
[5] W. G. Chen *et al.*, "Development of the heat treatment system for the 40 T hybrid magnet superconducting outsert," *Rev. Sci. Instrum.*, vol. 82, no. 10, 2011, Art. ID 105106.
[6] Y. F. Tan, W. G. Chen, Z. Y. Chen, P. He, and J. W. Zhu, "Characterization of Nb_3Sn strands for the model coil of the 40 T hybrid magnet," *IEEE Trans. Appl. Supercond.*, vol. 21, no. 4, pp. 3447–3450, Aug. 2011.
[7] J. A. Parrell, Y. Zhang, M. B. Field, and S. Hong, "Development of internal tin Nb_3Sn Conductor for Fusion and Particle Accelerator Applications," *IEEE Trans. Appl. Supercond.*, vol. 17, no. 2, pp. 2560–2563, Jun. 2007.
[8] A. K. Ghosh *et al.*, "Dynamic stability threshold in high-performance internal-tin Nb_3Sn superconductors for high field magnets," *Supercond. Sci. Technol.*, vol. 18, no. 1, pp. L5–L8, 2005.
[9] A. K. Ghosh *et al.*, "Magnetization studies of high Jc Nb_3Sn strands," *IEEE Trans. Appl. Supercond.*, vol. 15, no. 2, pp. 3494–3497, Jun. 2005.
[10] A. K. Ghosh *et al.*, "Effects of reaction temperature and alloying on performance of restack-rod-process Nb_3Sn," *IEEE Trans. Appl. Supercond.*, vol. 17, no. 2, pp. 2623–2626, Jun. 2007.
[11] H. Müller and Th. Schneider, "Heat treatment of Nb_3Sn conductors," *Cryogenics*, vol. 487, no. 7/8, pp. 323–330, 2008.